Biochimica et Biophysica Acta, 1145 (1993) 124–133
© 1993 Elsevier Science Publishers B.V. All rights reserved 0005-2736/93/$06.00

BBAMEM 75834

Orientation and structure of the NH_2-terminal HIV-1 gp41 peptide in fused and aggregated liposomes

Isabelle Martin, Fabienne Defrise-Quertain, Etienne Decroly, Michel Vandenbranden, Robert Brasseur and Jean-Marie Ruysschaert

Laboratoire de Chimie-Physique des Macromolécules aux Interfaces CP206 / 2, Université Libre de Bruxelles, Brussels (Belgium)

(Received 14 July 1992)

Key words: HIV; Fusion peptide; Lipid mixing; FTIR

For several retroviruses, the N-terminal hydrophobic sequence of the viral envelope glycoprotein has been shown to play a crucial role in the interaction between the virus and the host cell membrane. We report here on the interaction of a synthetic 16 residues peptide corresponding to the gp41 NH_2-terminal sequence of Human Immunodeficiency Virus with the phospholipid bilayer. Fluorescence energy transfer measurements show that this peptide can induce lipid mixing of large unilamellar vesicles (LUV) of various compositions at pH 7.4 and 37°C. LUV undergo fusion, provided they contained phosphatidylethanolamine (PE) in their lipid composition. To provide insight into the mechanism of the fusion event, the peptide secondary structure and orientation in the lipid bilayer were determined using Fourier Transform Infrared Spectroscopy (FTIR). The peptide adopts mainly a β-sheet conformation in the absence of lipids. After interaction with LUV the β-sheet is partly converted into α-helix. The orientation of the peptide with respect to the lipid acyl chains depends on the presence of PE in the lipid bilayer. The peptide is inserted into the lipid bilayer with the helix axis oriented parallel to the lipid acyl chains in the fused vesicles, whereas it is adsorbed parallel to the lipid/water interface in the aggregated vesicles. The role of the two kinds of orientation during the fusion event is discussed.

Introduction

Although a great deal of effort has been made to understand the genetic and immunological aspects of HIV infection, the molecular mechanism of fusion between the virus and its host cell remains poorly understood. Experimental evidence for the role of a viral envelope glycoprotein in membrane fusion has come from site-directed mutagenesis studies [1–4]. Many viral fusion proteins are synthesized as larger precursors and cleaved into two fragments: the external glycoprotein responsible for the virus attachment to the cell, and the transmembrane protein involved in the fusion mechanism. Most viral fusogenic proteins contain a short amino-terminal hydrophobic segment which has been proposed to interact with the lipid membrane during the fusion event [5,6]. For several retroviruses, mutagenesis studies have confirmed that this N-terminal hydrophobic sequence is critical for fusion to occur. Mutations which disrupt the distribution of the hydrophobic amino acids in the N-terminus of Influenza hemagglutinin [1], gp41 of HIV [2,4] and gp32 of SIV [3] inhibit syncytium formation without affecting glycoprotein synthesis and processing or receptor binding, suggesting that the hydrophobicity plays a key role in the fusion process.

A possible way to elucidate the molecular mechanism of membrane fusion is to synthesize peptides corresponding to the amino-terminus of viral fusion protein, and to study their interaction with model membranes. Synthetic peptides corresponding to the N-terminal segment of influenza (HA2) [7–10] have been shown to interact with the lipid bilayer and to promote fusion of lipid vesicles. Similar observations have been made with SIV and HIV fusion peptide [11,12].

Recent data suggest that the hydrophobicity of the N-terminal fusion peptide is not the only parameter required for fusion to occur and that the orientation and the secondary structure of the peptide at the lipid/water interface play a crucial role during the fusion event [13,14].

In this report, we examine the interaction of the HIV N-terminal 16 residues peptide with large unilamellar vesicles (LUV) of different compositions. The N-terminal peptide mediates either lipid aggregation

Correspondence to: I. Martin, Université Libre de Bruxelles, Campus Plaine CP 206/2, B-1050 Bruxelles, Belgium.

or lipid mixing depending on the phosphatidylethanolamine content of the lipid vesicles. Polarized FTIR spectroscopy allows the orientations of the N-terminal peptide to be determined in aggregated and fused vesicles. The data and analysis that are presented here provide evidence that these orientations are quite different before and after the fusion of the lipid vesicles.

Materials and Methods

Materials

Egg phosphatidylethanolamine (PE), egg phosphatidylcholine (PC), cholesterol (Chol), sphingomyelin (SM) were purchased from Sigma (St. Louis, USA).

Dioleoylphosphatidylcholine (DOPC), *N*-(7-nitrobenz2-oxa-1,3-diazol-4-yl)phosphatidylethanolamine (NBD-PE) and *N*-(lissamine Rhodamine B sulfonyl)phosphatidylethanolamine (Rh-PE) were from Avanti Polar Lipids (Birmingham, AL, USA).

8-Aminonaphthalene-1,3,6-trisulfonic acid sodium salt (ANTS) and *p*-xylylenebis(pyridinium) bromide (DPX) were from Molecular Probes (Junction City, OR).

The HIV16aa peptide is a gift from Dr. P. Horal (University of Göteborg, Sweden). The peptide was synthesized using the solid phase peptide synthesis and purity was checked by HPLC.

Methods

Vesicles preparation. Multilamellar vesicles (MLV) were obtained by vortexing a lipid film in a buffer (10 mM Tris, 150 mM NaCl, 0.1 mM EDTA, 0.02% NaN_3 (pH 7.4)).

Large unilamellar vesicles (LUV) were prepared according to the extrusion procedure of Hope et al. [15] using an Extruder (Lipex Biomembranes, Vancouver, Canada). Briefly, freezed and thawed MLV were extruded ten times through two stacked polycarbonate membranes with a pore size of 0.1 μm (Nucleopore, Pleasanton, CA, USA.).

Attenuated total reflection Infrared spectroscopy (ATR). Secondary structure determination: vibrational bands of protein or peptide, and particularly the Amide I band (1600–1700 cm^{-1}) are sensitive to the secondary structure [16]. This amide I band located in a region of the spectrum often free of other bands, is made out of 80% pure (C = O) vibration [17]. The strong overlaping of the different components of the amide I arising from the different secondary structures usually results in a broad, featureless envelope. The combination of resolution enhancement methods with a band fitting procedure allows the quantitative assessment of various components of protein or peptide secondary structure such as α-helix, β-sheet and unordered structures [18,19]. This procedure extended to a series of well characterized proteins provided a correct estimation of the α-helix and β-sheet structure content with a standard deviation of 8.7% when X-ray structures were taken as reference [20]. The percentages of the different secondary structure were quantified by an iterative curve-fitting. Each band was assigned to a secondary structure according to the frequency of its maximum. The area of all bands assigned to a given secondary structure were then summed up and divided by the total area. This ratio gives the proportion of the polypeptide chain in that conformation.

The frequency limits for each structure were first assigned according to the data determined theoretically [21] or experimentally [18]: 1662–1645 cm^{-1}, α-helix; 1689–1682 cm^{-1} and 1637–1613 cm^{-1}, β-sheet; 1644.5–1637 cm^{-1}, random; 1682–1662.5 cm^{-1}, β-turns. These limits have been slightly adjusted to obtain a good agreement between the proportion of each structure determined by IR-ATR and X-ray crystallography for a set of purified proteins [20].

Orientation determination: Attenuated Total Reflection Infrared Spectroscopy allows spectra to be recorded on ordered lipid bilayers and information to be gained about the orientation of different structures of protein or peptide [20]. In an α-helix, the main transition dipole moment (C = O) is almost parallel to the helix axis while in an antiparallel β-sheet the polarisation is opposite, predominantly perpendicular to the fiber axis [17]. It is therefore possible to determine the mean orientation of the α-helix and β-sheet structures from the orientation of the peptide bond corresponding to the C = O group. Spectra were recorded with parallel (0°) and perpendicular (90°) polarized incident light with respect to the ATR plate. Polarization was expressed as the dichroic ratio $R_{atr} = A_{90°}/A_{0°}$. The mean angle between the C = O band and a normal to the ATR plate surface is calculated from R_{atr} as described in Cabiaux et al. [22].

Spectra were recorded with a Perkin Elmer infrared spectrophotometer FTIR 1720X equipped with a Perkin Elmer microspecular reflectance accessory (ref. P.E 221–0357) and a polarizer mount assembly with a silver bromide element (ref. P.E.L 106–0249). The internal reflection element was a Germanium plate (50 × 20 × 2 mm) with an aperture angle of 45°, yielding 25 internal reflections. 128 scans cycles were averaged. In each cycle, the sample spectra were ratioed against the average of the background spectra of a clean germanium plate. For polarization experiments, a Perkin Elmer gold wire grid polarizer was positioned before both the sample and the reference plate.

Sample preparation. HIV peptides dissolved in DMSO at a final concentration of 1 mg/ml, were added to liposomes (molar lipid/peptide ratio of 300 : 1) ($2.9 \cdot 10^{-6}$ M of lipid and 10^{-8} M of peptide in a total volume of 200 μl). After 3 h incubation at 37°C,

aggregated and/or fused liposomes mixed with an equal volume of 80% sucrose were deposited on a flotation sucrose gradient (30%–2%) to separate the lipid-peptide complex from the free peptides or the free liposomes. After centrifugation (Ultracentrifuge Beckman L765) at 35000 rpm and 4°C for 16 h in a SW60 Beckman rotor, the gradient was fractionated and the fractions were tested for the presence of PC using the enzymatic colorimetric test of Boehringer-Mannheim. Liposomes were collected and dialyzed on Centricon 30 against tridistilled water to eliminate the excess of sucrose and salts which could interfere in the IR analysis. Oriented multilayers were obtained by slow evaporation of the liposomes under N_2 on one side of the germanium plate. To differentiate between the α-helix and the random structures, the multilayers were exposed 3 h to D_2O-saturated N_2 [22].

Lipid mixing assay. Lipid mixing was determined by measuring the fluorescence intensity change resulting from the fluorescence energy transfer between the probes NBD-PE and Rh-PE, as described by Struck et al. [23]. Fluorescence was monitored using a SLM 8000 spectrofluorimeter with excitation and emission slits of 4 nm. Both probes were added to the lipid film and LUV were prepared as described above.

Liposomes containing both probes at 0.6% (molar ratio) each, were mixed in a 1:9 mol ratio with probe free liposomes at a final lipid concentration of $3 \cdot 10^{-4}$ M. The initial fluorescence of the 1:9 (labeled/unlabeled) suspension was taken as 0% fluorescence and the 100% fluorescence was determined using an equivalent concentration of vesicles prepared with 0.06% of each fluorescent phospholipid. The suspensions were excited at 470 nm and the NBD fluorescence was recorded at 530 nm.

Leakage assay. The ANTS/DPX assay of Ellens et al. [24] was used to monitor vesicle leakage. The assay is based on the quenching of ANTS by DPX. ANTS and DPX are coencapsulated in the aqueous phase of one population of liposome. Leakage of lipid vesicles contents induced by interaction with the peptides was followed by measuring the dequenching of ANTS released into solution [24]. Fluorescence was monitored using a spectrofluorimeter SLM 8000 with excitation and emission slits of 4 nm.

Liposomes (LUV) were prepared as described above in 12.5 mM ANTS, 45 mM DPX, 65 mM NaCl, 10 mM Tris-HCl at pH 7.4. Vesicles containing encapsulated ANTS and DPX were chromatographied on a Sephadex G-75 column, eluted with 10 mM Tris-HCl, 150 mM NaCl (pH 7.4), to remove unencapsulated material from the vesicle suspension.

The liposomal lipid concentrations were determined by phosphate analysis [25]. Fluorescence of liposome at a final lipid concentration of $3 \cdot 10^{-4}$ M corresponds to 0% leakage. 100% leakage was the fluorescence after lysis of the vesicles with Triton X-100 (20 μl of TX-100 10% in H_2O). Samples were excited at 360 nm, emission was measured at 520 nm.

Aqueous contents mixing assay. The assay is based on the quenching of ANTS by DPX. ANTS is encapsulated in the inner aqueous phase of one population of liposomes and DPX in the other. Mixing of the inner aqueous contents of liposomes results in quenching of ANTS fluorescence [24].

Large unilamellar vesicles (LUV) were prepared as described above, and contained 25 mM ANTS and 89 mM NaCl or 90 mM DPX and 39 mM NaCl. All solutions were buffered with 10 mM Tris-HCl at pH 7.4. The liposomes were separated from unencapsulated material on Sephadex G-75 in 10 mM Tris-HCl, 150 mM NaCl (pH 7.4) buffer. Liposomal lipid concentrations were determined by phosphate analysis [25]. Fluorescence was monitored using a spectrofluorimeter SLM 8000 with excitation and emission slits of 4 nm.

Mixing of aqueous contents of ANTS and DPX containing liposomes is registered as a decrease in ANTS fluorescence due to quenching by DPX. The fluorescence of a 1:1 mixture of ANTS and DPX liposomes in Tris-HCl buffer, correspond to 0% fusion. The 100% fusion was the residual fluorescence of liposomes containing 12.5 mM ANTS and 45 mM DPX. Excitation wavelength was 360 nm, emission was measured at 520 nm.

Results

We report here about the interaction between a 16 amino acids synthetic peptide (HIV16aa) corresponding to the fusogenic sequence of the HIV gp41 and large unilamellar vesicles (LUV). Their curvature and stability better mimic the cell membrane as compared to small unilamellar vesicles (SUV) whose small radius of curvature perturbs the lipid organization. Although fusion events observed with SUV system do reveal peptide-induced bilayer destabilization, they do not necessary reflect the intrinsic fusogenicity of the peptide [10].

HIV16aa sequence (HIV_{HXB2}):

Ala-Val-Gly-Ile-Gly-Ala-Leu-Phe-Leu-Gly-Phe-Leu-Gly-Ala-Ala-Gly

Lipid mixing

Lipid mixing of LUV was monitored by resonance energy transfer [23]. Addition of the HIV peptide to LUV of PC/PE/SM/Chol (1:1:1:1.5 molar ratio) induces a lipid mixing between labeled and unlabeled vesicles. The process is fast and fusion reaches its maximal value after less than 4 min (Fig. 1).

The replacement of PE with PC (PC/SM/Chol 2:1:1.5 molar ratio) completely inhibits the lipid mix-

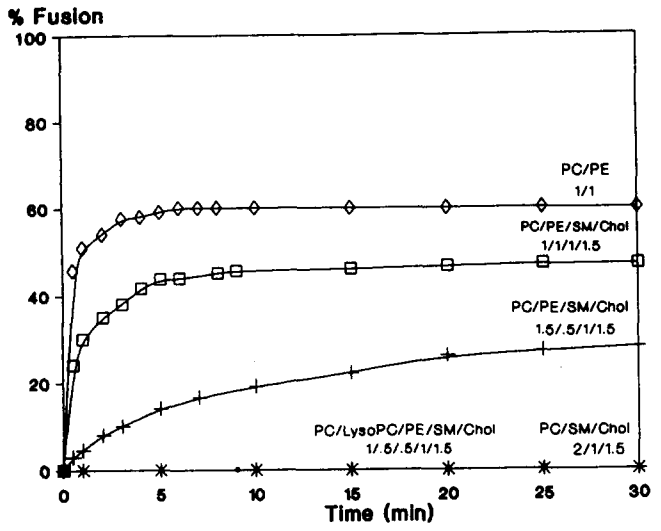

Fig. 1. Fusion of large unilamellar vesicles (LUV) induced by the HIV16aa peptide at various lipid compositions (the represented curve is an average of five independent experiments and the error on the fusion percentage is 2%). Labeled and unlabeled vesicles were mixed at a 1:9 ratio. At time 0, the peptide in DMSO was added and the increase of fluorescence, due to a decrease in fluorescence energy transfer following liposome-liposome fusion was monitored at 530 nm, pH 7.4 and 37°C. Dimethylsulfoxide (DMSO) up to 2% (v/v), which is the maximal concentration used, did not modify the fluorescence. The experimental conditions were the same for all the lipid compositions tested. The total lipid concentration was $3 \cdot 10^{-4}$ M and the peptide concentration $1.3 \cdot 10^{-5}$ M. The molar lipid/peptide ratio is 25.

ing (Fig. 1). PE has been shown to form non lamellar lipid structures [26] and to enhance the fusion process when it is inserted in the lipid bilayer. In order to better define the role of PE in the fusion process, a fraction of PE was replaced with lysophosphatidylcholine. Fusion did not occur after addition of HIV16 to LUV of PC/lysoPC/PE/SM/Chol (1:0.5:0.5:1:1.5, molar ratio). This inhibition was not the consequence of an insufficient amount of PE, since HIV16aa triggers lipid mixing of PC/PE/SM/Chol LUV (1.5:0.5:1:1.5 molar ratio) (Fig. 1) when lysophosphatidylcholine was replaced with a corresponding amount of PC. The inhibition effect observed could be interpreted in term of molecular 'shape': lysophosphatidylcholine adopts a conical shape complementary to that of PE [27] and in an equimolar mixture of lysoPC and unsaturated PE, lysoPC stabilises the bilayer organization [28]. Moreover, Fig. 1 suggests that the overall PC to PE ratio modulates the fusogenic activity.

The HIV16aa peptide-induced fusion is temperature dependent between 20°C and 45°C (Fig. 2). This effect is PE specific and is not observed with SUV of DOPC. DOPC SUV were used for comparison since no lipid mixing could be observed for DOPC LUV (data not shown). The mixing of the lipid phases increases steeply between 30°C and 40°C. It is in this temperature range that the transition of PE from a bilayer to a non lamellar lipid structures occurs. Hong et al. [29] determined this transition temperature for MLV of eggPE between 38°C and 43°C. It should nevertheless be kept in mind that this transition temperature could be broadened in vesicules with more complex compositions. The increase in fusion observed between 5 and 20°C does not depend on the lipid composition and can obviously not be explained in terms of hexagonal phases formation.

Aqueous contents mixing and leakage of aqueous contents

Mixing of both lipid and aqueous contents should be observed in an ideal fusion process. The mixing and/or leakage of aqueous contents of the liposomes were monitored using the ANTS-DPX assay developped by Ellens et al. [24]. Briefly, for leakage experiments, fluorophore (ANTS) and quencher (DPX) are co-encapsulated in the vesicles. Fluorescence increase demonstrates the release of vesicles contents into the external medium. For aqueous contents mixing, liposomes containing ANTS are mixed with liposomes containing DPX. Mixing of inner aqueous contents occuring during vesicles fusion causes a decrease in fluorescence intensity.

Addition of the HIV16aa peptide to LUV PC/PE/SM/Chol containing co-encapsulated ANTS and DPX, induces a rapid increase of the fluorescence demonstrating the fast leakage of internal contents (Fig. 3). This leakage explains why addition of HIV16aa peptide to a mixture of liposomes containing ANTS and liposomes containing DPX did not modify the ANTS fluorescence (data not shown).

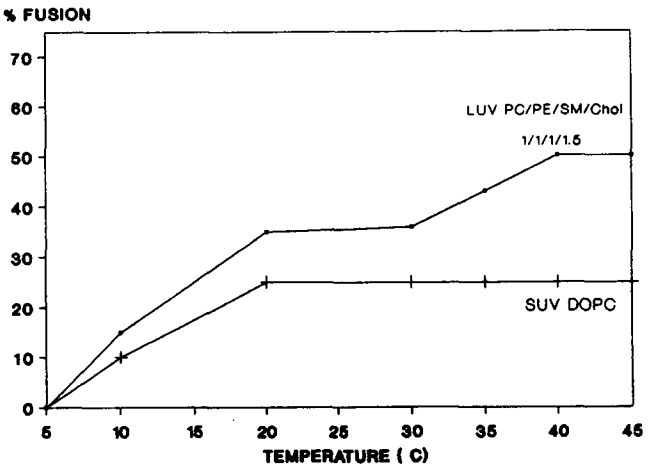

Fig. 2. Effect of temperature on lipid mixing of LUV induced by 13 μM of HIV16aa.The percentage of fusion was calculated 10 min after addition of peptide ($1.3 \cdot 10^{-5}$ M) to vesicles ($3 \cdot 10^{-4}$ M) suspended in Tris-HCl buffer at pH 7.4 and 37°C. The molar lipid/peptide ratio is 25. Fusion data are the average of three independent measurements.

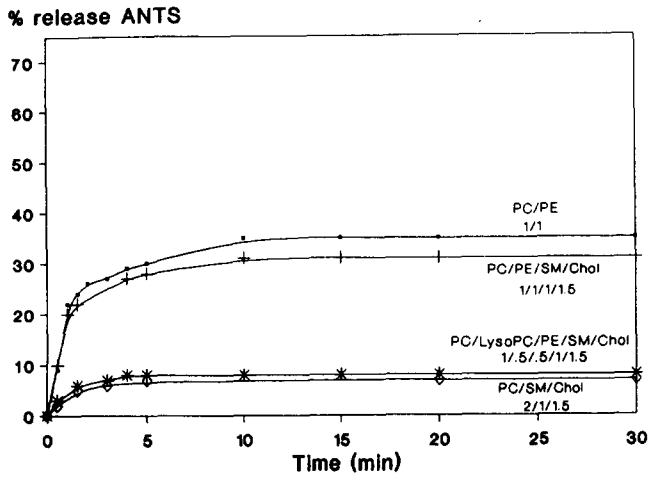

Fig. 3. Leakage of aqueous contents of LUV monitored with the ANTS/DPX assay at neutral pH and 37°C (the represented curve is an average of five independent experiments and the error on the fusion percentage is 2%). 13 μM of HIV16aa peptide was added at $t = 0$ in $3 \cdot 10^{-4}$ M ANTS/DPX liposomes suspended in Tris-HCl buffer at pH 7.4. Increase of fluorescence due to the dilution of ANTS in the suspension was monitored at 520 nm.

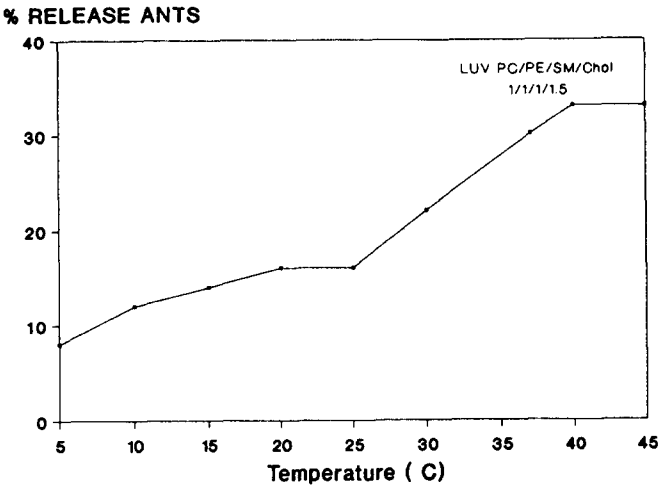

Fig. 4. Effect of temperature on leakage of aqueous content of LUV of PC/PE/SM/Chol (1:1:1:1.5, molar ratio) induced by 13 μM of HIV16aa. The percentage of leakage was calculated 10 min after addition of peptide ($1.3 \cdot 10^{-5}$ M) to vesicles ($3 \cdot 10^{-4}$ M) suspended in Tris-HCl buffer at pH 7.4 and 37°C. The molar lipid/peptide ratio is 25. Leakage data are the average of three independent measurements.

The peptide-induced leakage depends on the lipid composition of the vesicles. It was extensive with liposome containing PE (PC/PE/SM/Chol or PC/PE), whereas in the absence of PE (PC/SM/Chol or DOPC) only a small percentage of leakage was observed ($\pm 10\%$). Addition of lysophosphatidylcholine to LUV of PC/PE/SM/Chol inhibited totally the release (Fig. 3).

As demonstrated in the lipid mixing assay, the ability of HIV16aa peptide to promote leakage of ANTS-DPX from LUV is temperature dependent (Fig. 4).

The fast PE dependent leakage could be associated to the formation of non lamellar lipid structures during the fusion event. The formation of these transient lipid structures is expected to result in a loss of vesicle integrity and a concomitant release of the enclosed content.

Conformational studies

The FTIR spectra of HIV16aa peptide dissolved in DMSO reveal a high content of β-sheet structure (Table I, Fig. 6). After incubation with LUV of PC/PE/SM/Chol (1:1:1:1.5 molar ratio) or LUV of PC/SM/Chol (2:1:1.5 molar ratio) at a lipid/peptide molar ratio of 300 during 3 h at 37°C, the vesicles were isolated by density gradient centrifugation (2%–30% sucrose gradient). The vesicles loaded with HIV16aa concentrate in the middle of the gradient whereas free liposomes migrate to the top (Fig. 5) and free peptide remains at the bottom of the tube. IR spectra of proteoliposomes were recorded after removal of sucrose by dialysis. The amount of HIV peptide associated to the lipid is difficult to evaluate by colorimetric methods because of the small amount of an hydrophobic peptide, and the presence of lipids. To estimate the proportion of peptide associated to the lipid vesicles in the two systems (with and without PE), the peptide/lipid ratio was determined by measuring the ratio $S_{amide}/S_{\nu(C=0)lipid}$ on the IR spectra (S_{amide} is the area of amide I measured between 1680 cm^{-1} and 1600 cm^{-1}, and $S_{\nu(C=0)lipid}$ is the area of the lipid $\nu(C=0)$ band between 1770 cm^{-1} and 1700 cm^{-1}) [20]. In the two systems the ratios $S_{amide}/S_{\nu(C=0)lipid}$ were identical for equal lipid concentrations (data not shown), suggesting that the same amount of peptide is associated to the vesicles in the presence and in the absence of PE in the lipid bilayer.

IR spectra of the proteoliposomes (with and without PE) show that in contrast to lipid-free peptide the lipid-associated peptide displays some α-helical structure (Fig. 6, Table I) characterized by the appearance of a new large peak centered around 1650 cm^{-1}. This significant increase of the α-helix ($\pm 25\%$) content is

TABLE I

Proportion of the different secondary structures of HIV16aa in the absence and in the presence of lipid

The molar lipid/peptide ratio is 300. The percentage of structure is the average of three independent measurements.

Sample	α-helix	β-sheet	Random	β-turn
HIV16aa	0%	99% ± 5%	0%	0%
LUV PC/PE/SM/Chol	25% ± 4%	41% ± 5%	28% + 5%	6%
LUV PC/SM/Chol	25% ± 4%	50% + 5%	25% ± 5%	0%

accompanied by a decrease of the β-sheet content (Table I). These structural changes observed for LUV of PC/PE/SM/Chol and LUV of PC/SM/Chol are identical (Table I).

The spectra of HIV16aa inserted into LUV of PC/PE/SM/Chol (1:1:1:1.5 molar ratio) and LUV of PC/SM/Chol (2:1:1.5 molar ratio) were recorded with parallel (0°) and perpendicular (90°) polarized light. The difference spectra 90°–0° (Fig. 7) show a negative deviation around 1657 cm^{-1} for the helical structure associated to the aggregated LUV of PC/SM/Chol which characterizes an orientation of the helix axis parallel to the ATR element surface. The deviation is positive for the α-helix associated to the fused LUV of PC/PE/SM/Chol indicating an orientation normal to the ATR element surface (Fig. 7). The curve fitting applied to the polarized spectra in the amide I region allows the evaluation of the dichroic ratio for the α-helical structure. From this, it is possible to calculate a corresponding angle between the long axis of the α-helix and a normal to the germanium plate. For the helical structure associated to the LUV of PC/SM/Chol the angle is equal to 70° ± 5° and to 5° ± 5° for LUV of PC/PE/SM/Chol. To determine these orientations, a 27° deviation angle between the α-helix axis and the C = O transition dipole moment described by Rothschild et al. [43] was taken into account by introducing an order parameter $S_{C=O} = (3\cos^2 27° - 1)/2$ so that $S_{helix} = S_{measured}/S_{C=O}$ [20,22]. The angle between the helix axis and the perpendicular to the bilayer we arrive at is therefore a minimum estimate and an orientation of the helix axis closer to this perpendicular would result from considering other sources of disorder such as an imperfect parallelism between the bilayer and the germanium crystal surface. Dichroic ratios corresponding to the β-sheet structure revealed no significant orientation.

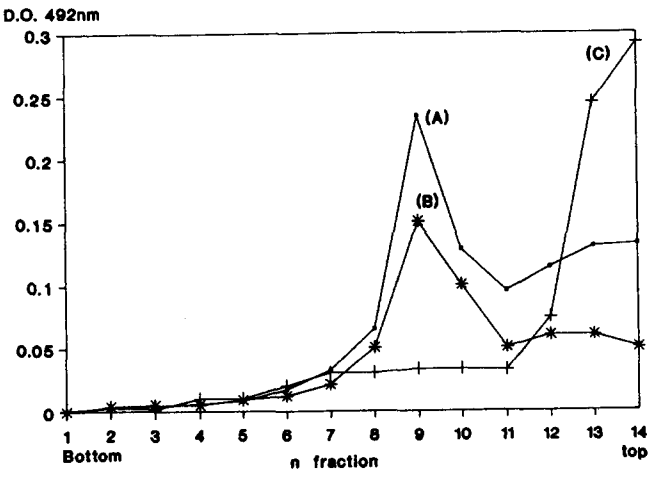

Fig. 5. Dosage of lipids by an enzymatic colorimetric test specific for choline in (A) HIV16aa/LUV PC/PE/SM/Chol (1:1:1:1.5, molar ratio), (B) HIV16aa/LUV PC/SM/Chol (2:1:1.5, molar ratio) and (C) LUV PC/PE/SM/Chol (1:1:1:1.5, molar ratio) samples after centrifugation on a continuous sucrose 2%–30% density gradient.

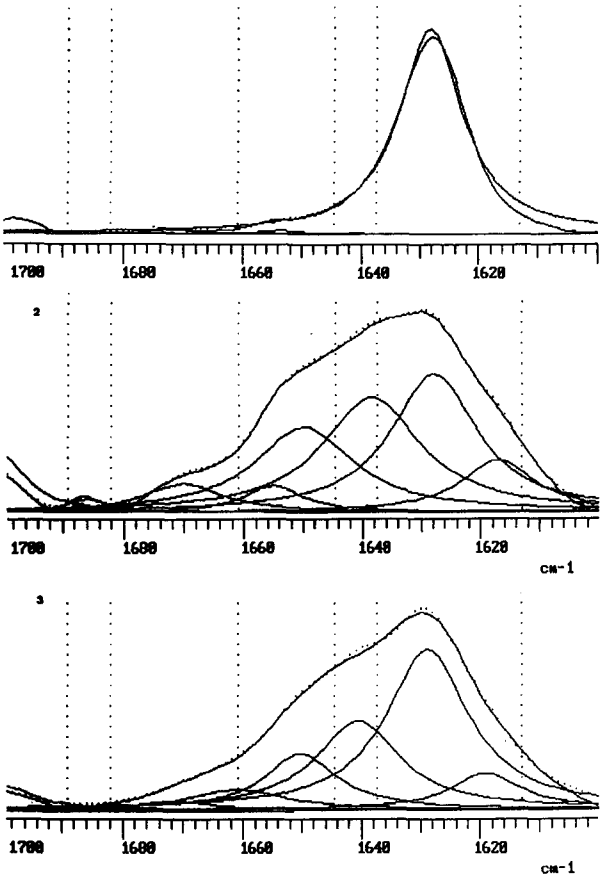

Fig. 6. Curve fitting of the amide I region of the HIV16aa peptide (1) in DMSO, (2) incubated with LUV PC/PE/SM/Chol (1:1:1:1.5, molar ratio), (3) incubated with LUV PC/SM/Chol (2:1:1.5, molar ratio). HIV16aa was incubated with LUV in a molar lipid/peptide ratio of 300 (2 mg of lipid in a total volume of 200 μl). The sample were deuterated 2 h. The result of the fitting appears under the curve. The vertical dotted lines define the region of the spectrum assigned to the different secondary structures. The frequency limits were as follows: 1662–1645 cm^{-1}, α-helix; 1689–1682 cm^{-1} and 1637–1613 cm^{-1}, β-sheet; 1644.5–1637 cm^{-1}, random; 1682–1662.5 cm^{-1}, βturns. The sum of the spectral components is represented by the dotted spectrum.

To confirm that these different orientations are not due to a difference in the overal membrane orientation on the germanium plate, we have characterized the orientation of the phospholipids of the bilayer (Fig. 7). In lipid bilayers, the transition dipole moment of the γw (CH2) peak at 1200 cm^{-1} lies along the hydrocarbon chains; this band was therefore chosen to characterize the lipid acyl chain orientation. The dichroic spectra 90°–0° show a positive deviation at 1200 cm^{-1} indicating that the lipid chains in LUV of PC/SM/Chol (Fig. 7B) and LUV of PC/PE/SM/Chol (Fig. 7A) are oriented preferentially perpendicular to the germanium surface. This orientation is confirmed in the dichroic spectra by the negative deviation observed

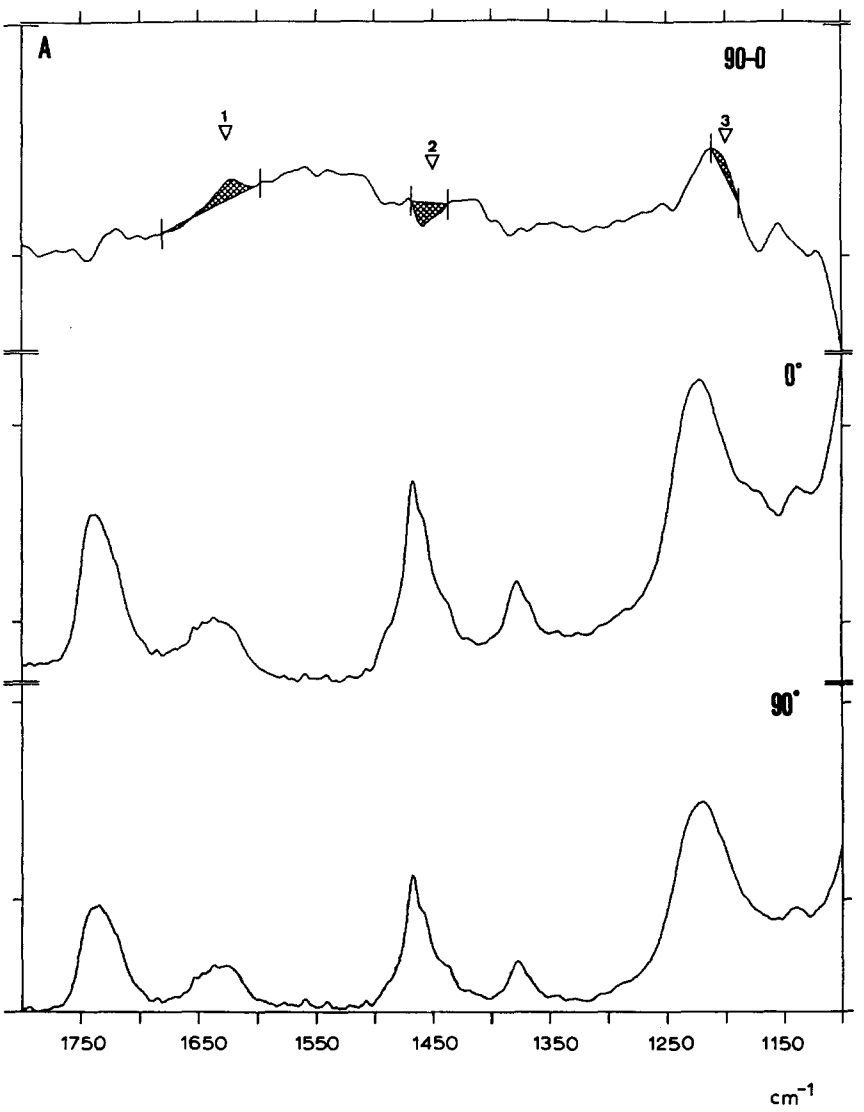

Fig. 7. ATR spectra of HIV16AA inserted in LUV PC/PE/SM/Chol (A) and LUV PC/SM/Chol (B), recorded using 90° and 0° polarization. The dichroism spectrum obtained by subtracting the (90°–0°) recorded spectra is plotted on the top of the figure, expanded 3-fold in the ordinate direction. The arrows indicate the protein amide I, the phospholipid δ(CH2) at 1468 cm^{-1} and the γ(CH2) at 1200 cm^{1}.

near 1468 cm^{-1} corresponding to the δ (CH2) peak whose transition dipole moment is perpendicular to the axis of the lipid chains.

Discussion

The synthetic 16-residues peptide corresponding to the gp41 N-terminus of HIV triggers the mixing of lipid bilayers, which is accompanied by a change in membrane permeability: small solutes (like ANTS and DPX) rapidly leak out of the vesicles as observed for fusogenic peptides of influenza [9], HIV [12] and SIV [11]. The kinetics of the two processes are similar suggesting that the leakage observed is associated to non lamellar lipid structures formation or local change in the lipid bilayer organization caused by the peptide.

We did obviously not demonstrate that the structure of the isolated peptide is the one adopted in the entire protein. This would require a knowledge of the three-dimensional structure of the envelope glycoprotein in its lipidic environment. Such a detailed representation will probably not be accessible in the near future.

Whereas the N-terminal domain seems to play a central role in the virus/cell fusion process, other domains might play a role as well. In HIV-1, mutations in the third hypervariable region of the external glycoprotein, the V3 loop, inhibit the syncytia formation without affecting the capacity of gp160 to bind to its receptors [2,4]. Several neutralizing antibodies against the V3 loop, which is the major immunogenic epitope of HIV-1, inhibit viral penetration without affecting the attachment of the virus to its receptor. This post

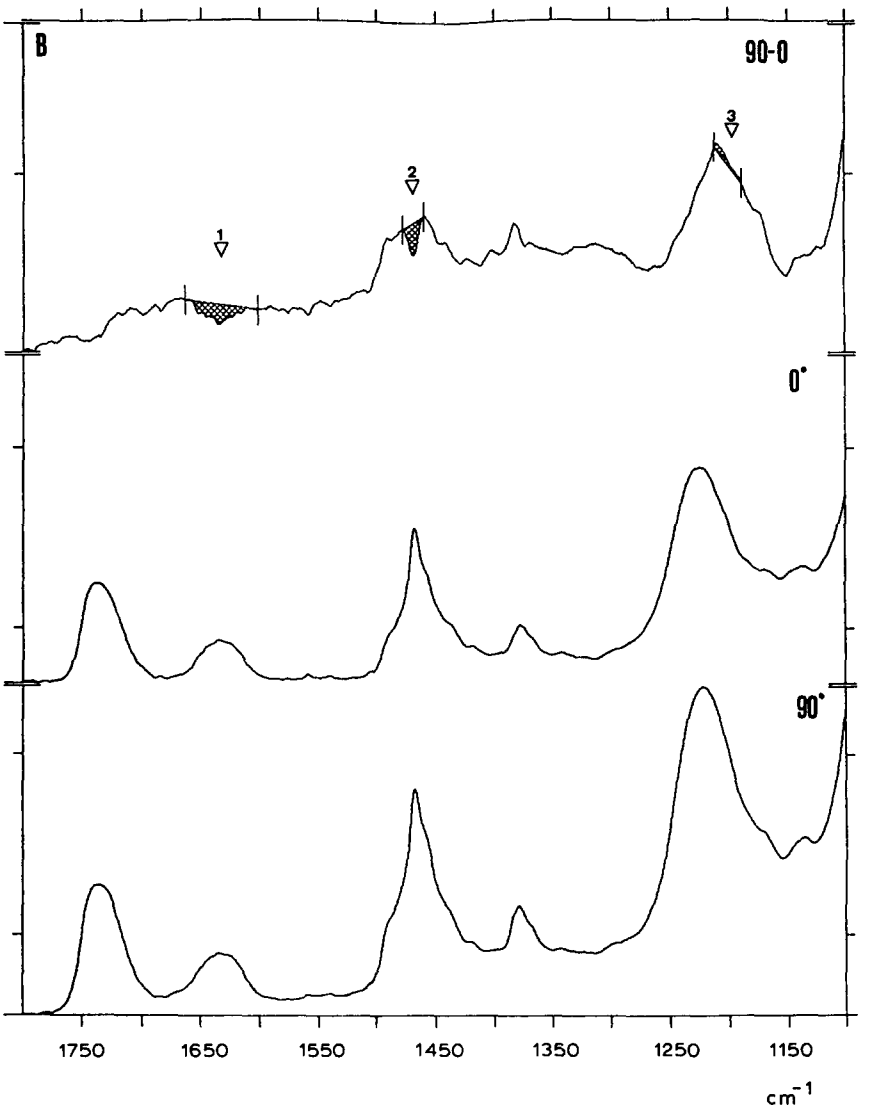

Fig. 7 (continued).

binding neutralization is thought to act at the level of the fusion step [30,31].

Although it has become obvious that fusion peptide plays an essential role in the fusion event, the membrane lipids must be actively involved. It is difficult to imagine that the lipid bilayer structure is preserved during this process.

PE is known to form non lamellar lipid structures. A relationship between non lamellar lipid structures formation (H_{II}) and the fusion process has been proposed [32]. A number of examples of structurally different compounds (cholesterol sulfate [33], carbobenzoxy-D-Phe-L-Phe-Gly [34], tromantadine [35]...) that are bilayer stabilizers and show antiviral activity, and the demonstration that some of these agents inhibit both model membrane as well as viral fusion, suggest that there is a relationship between the effect of these drugs on the lipid structure and their antiviral activity. There are many potential sites of action for these bilayer stabilizers, but their antiviral activity results from a change in the biophysical properties of the lipid membrane and in some cases, in the increase of the bilayer/non lamellar lipid structures transition temperature [46].

In our study, differents experimental arguments seem to be in favor of the formation of an H_{II} phase structure during the fusion event. (1) The presence of PE in the lipid bilayer enhances the fusion process and the fusogenic activity is significantly increased in the range of the PE H_{II} transition temperature (37°C–45°C). In the experimental conditions used PE may form a non lamellar lipid structure but we have no direct proof of the involvement of this phase in the fusion process induced by HIV16aa.

(2) Lysophosphatidylcholine inhibits the mixing of the lipid phases of LUV of PC/lysoPC/PE/SM/Chol (1:0.5:0.5:1:1.5 molar ratio). This lipid with a large polar head group has a conical shape complementary

to the inverted conical shape of PE at 37°C [28]. In an equimolar mixture of lysoPC/PE, lysoPC stabilizes the lipid organization and increases the temperature of transition from a bilayer to a non lamellar lipid structures transition [28].

In the second part of this study, we attempted to correlate the fusogenic activity of the HIV16aa peptide with its mode of insertion into the lipid bilayer. Determination of the conformation of membrane proteins by experimental means has been challenged by the difficulties encountered in obtaining crystals of proteins suitable for high resolution X-ray crystallography and by the turbidity inherent to membrane fragments which prevent them from being analyzed by spectroscopy methods using ultraviolet or visible light. IR spectroscopy has been shown to be applicable to membrane proteins [36,22,38]. The analysis of the IR data is based on the hypothesis that the formation of a thin hydrated film does not modify the secondary structure [20]. Determination of the protein structures by transmission in solution and attenuated total reflection yielded similar results, indicating that the drying-rehydration cycle experienced by the sample on the ATR plate did not significantly modify the secondary structure of the protein. This analysis has been carried out for apo-B100 [38] and for small peptides such as the 21 amino acids signal peptide of PhoE [44].

The HIV fusogenic peptide undergoes a conformational transition from β-sheet to more α-helix when interaction with lipids occurs. This increase in the helical content in a lipid environment has been established for viral peptides corresponding to the NH_2-terminus of influenza [7], SIV [11], for signal peptides [45] and for the GALA peptide [36].

Analysis of the polarized spectra brings evidence that the orientation of the α-helix axis depends on the presence of PE in the lipid bilayer. With PE in the lipid bilayer, the α-helix axis is oriented parallel to the lipid chains, whereas in the absence of PE the α-helix is parallel to the lipid/water interface suggesting its non insertion in the membrane. No significant orientation could be demonstrated for the β-sheet conformation. At the lipid/water interface, the helix orientation is stabilized as well by polar interactions between the hydrophilic side of the helix and the aqueous medium as by hydrophobic interactions between the hydrophobic side of the helix and the lipid acyl chains. About the peptide inserted into the lipid bilayer, computer simulation shows that three or four α-helix oriented normal to the lipid/water interface could self-associate to form a transmembrane structure into the bilayer (Brasseur, R., personal communication).

It should be kept in mind that when peptide is added to the liposome suspension, peptide-peptide interactions could be favored with respect to peptide-lipid interactions. It is not clear how such interactions contribute to the fusogenic activity, and further experimental data are required to separate the contribution associated to peptide self-association and binding of peptide to the bilayer.

The data reported here suggest that the membrane insertion of the HIV fusion peptide plays an important role in vesicle fusion and in virus-cell membrane fusion. It has been proposed that the fusion process involves the penetration of the fusion peptide into the target membrane [5,41,6].

Acknowledgments

This work was performed with the financial support of BNB (Banque Nationale de Belgique), CGER (Caisse Générale d'Epargne et de Retraite), FNRS (Fonds National de la Recherche Scientifique), IRSIA (Institut pour l'Encouragement de la Recherche Scientifique dans l'Industrie et l'Agriculture) and Smith Kline Beecham Biologicals. One of us (R.B.) is Senior Research Associate of the National Fund for Scientific Research. We gratefully thank NIH (NIAID grant A1-27136-01A1) and the Commission of the European Communities (SC 1000195) for continued financial support.

References

1 Gething, M.-J., Doms, R., York, D. and White, J. (1986) J. Cell Biol. 102, 11-23.
2 Kowalski, M., Potz, J., Basiripour, L., Dorfman, T., Goh, W., Terwilliger, E., Dayton, A., Rosen, C., Haseltine, W. and Sodroski, J. (1987) Science 237, 1351-1355.
3 Bosch, M., Earl, P., Fargnoli, K., Picciafuoco, S., Giombini, F., Wong Staal, F. and Franchini, G. (1989) Science 244, 694-697.
4 Freed, E.O. and Risser, R. (1990) Bull. Inst. Pasteur 88, 73-110.
5 Harter, C., James, P., Bächi, T. and Brunner, J. (1989) J. Biol. Chem. 264, 6459-6464.
6 Brunner, J., Zugliani, C. and Mischler, R. (1991) Biochemistry 30, 2432-2438.
7 Lear, J.D. and DeGrado, W. (1987) J. Biol. Chem. 262, 6500-6505.
8 Murata, M., Sugahara, Y., Takahashi, S. and Ohnishi, S. (1987) J. Biochem. 102, 957-962.
9 Wharton, S.A., Martin, S., Ruigrok, R., Skehel, J. and Wiley, D. (1988) J. Gen. Virol. 69, 1847-1857.
10 Rafalski, M., Ortiz, A., Rockwell, A., Van Ginkel, L., Lear, J., DeGrado, W. and Wilschut, J. (1991) Biochemistry 30, 10211-10220.
11 Martin, I., Defrise-Quertain, F., Mandieau, V., Nielsen, N.M., Saermark, T., Burny, A., Brasseur, R., Ruysschaert, J.M. and Vandenbranden, M. (1991) Biochem. Biophys. Res. Commun. 175, 872-879.
12 Rafalski, M., Lear, J. and DeGrado, W. (1990) Biochemistry 29, 7917-7922.
13 Horth, M., Lambrechts, B., Marinee, C., Bex, F., Thiriart, C., Ruysschaert, J.-M., Burny, A. and Brasseur, R. (1991) EMBO J. 10, 2747-2755.
14 Vonèche, V., Portetelle, D., Kettman, R., Willems, L., Limbach, K., Paoletti, E., Ruysschaert, J.M., Burny, A. and Brasseur, R. (1992) Proc. Natl. Acad. Sci. USA 89, 3810-3814.

15 Hope, M.J., Bally, M.B., Webb, G. and Cullis, P.R. (1985) Biochim. Biophys. Acta 812, 55–65.
16 Fringeli, U.R. and Günthard, M.H. (1981) in Membrane Spectroscopy (Grell, E., ed.), pp. 270–332, Springer.
17 Gremlich, H.U., Fringeli, U. and Schwyzer, R. (1983) Biochemistry 22, 4257–4264.
18 Byler, D.M. and Susi, H. (1986) Biopolymers 25, 459–487.
19 Kauppinen, J.K., Moffat, D.J., Cameron, D.G. and Mantsch, H. (1981) Appl. Opt. 20, 1866–1879.
20 Goormaghtigh, E., Cabiaux, V. and Ruysschaert, J.-M. (1990) Eur. J. Biochem. 193, 409–420.
21 Krimm, S. and Bandekar, J. (1986) Adv. Protein Chem. 38, 181–364.
22 Cabiaux, V., Brasseur, R., Wattiez, R., Falmagne, P., Ruysschaert, J.-M. and Goormaghtigh, E. (1989) J. Biol. Chem. 264, 4928–4938.
23 Struck, D.K., Hoekstra, D. and Pagano, R. (1981) Biochemistry 20, 4093–4099.
24 Ellens, H., Bentz, J. and Szoka, F.C (1984) Biochemistry 23, 1532–1538.
25 Msrny, R.J., Volwerk, J.J. and Griffith, O.H. (1986) Lipids 39, 187–191.
26 Verkleij, J. (1984) Biochim. Biophys. Acta 779, 43–63.
27 De Kruijff, B., Cullis, P.R., Verkleij, A.J., Hope, M.J., Van Echteld, C. and Taraschi, T.F. (1984) in Enzymes of biological membranes (Martinosi, A., ed.), Plenum, New York.
28 Maddon, T. and Cullis, P.(1982) Biochim. Biophys. Acta 684, 149–153.
29 Hong, K., Baldwin, P., Allen, T. and Papahadjopoulos, D. (1988) Biochemistry 27, 3947–3955.
30 Skinner, M., Langlois, A., Mcdanal, C., McDougal, S., Bolognesi, D. and Matthews, T. (1988) J. Virol. 62, 4195–4200.
31 Looney, D., Hayashi, S., Nicklas, M., Redfield, R., Broder, S., Wong-Staal, F. and Mitsuya, H. (1990) J. AIDS 3, 649–657.
32 Ellens, H., Siegel, D., Alford, D., Yeagle, P., Boni, L., Lis, L., Quinn, P. and Bentz, J. (1989) Biochemistry 28, 3692–3703.
33 Cheetman, J.J., Wachtel, E., Bach, D. and Epand, R.M. (1989) Biochemistry 28, 8929–8934.
34 Epand, R.M. (1986) Biosci. Rep. 6, 647–653.
35 Cheetman, J.J. and Epand, R.M. (1987) Biosci. Rep. 7, 225–230.
36 Goormaghtigh, E., De Meutter, J., Szoka, F., Cabiaux, V., Parente, R. and Ruysschaert, J.-M. (1991) Eur. J. Biochem. 195, 421–429.
37 Martin, I., Defrise-Quertain, F., Nielsen, N., Saermark, T., Burny, A., Brasseur, R., Vandenbranden, M. and Ruysschaert, J.-M. (1992) In Advances in Membrane Fluidity, Vol. 6 (Aloia, R., Curtain, C. and Gordon, L., eds.), pp. 365–376.
38 Goormaghtigh, E., De Meutter, J., Vanloo, B., Brasseur, R., Rosseneu, M. and Ruysschaert, J.-M. (1989) Biochim. Biophys. Acta 1006, 147–150.
39 Brasseur, R., Vandenbranden, M., Cornet, M., Burny, A. and Ruysschaert, J.-M. (1990) Biochim. Biophys. Acta 1029, 267–273.
40 Brasseur, R. (1991) J. Biol. Chem. 266, 16120–16127.
41 Harter, C., James, P., Bächi, T., Semenza, G. and Brunner, J. (1988) Biochemistry 27, 1856–1864.
42 Bentz, J., Ellens, H. and Alford, D. (1990) FEBS Lett. 276, 1–5.
43 Rothschild, K., Sanches, R., Hsiao, T. and Clark, N. (1980) Biophys. J. 31, 53–60.
44 Demel, R.A., Goormaghtigh, E. and De Kruijff, B. (1990) Biochim. Biophys. Acta 1027, 155–162.
45 Goormaghtigh, E., Martin, I., Vandenbranden, M., Brasseur, R. and Ruysschaert, J.-M. (1989) Biochem. Biophys. Res. Commun. 158, 610–615.
46 Epand, R.M. (1990) Biochem. Cell. Biol. 68, 17–22.